

CALIBRATION OF A GEOTHERMAL MODEL USING PEST

Racquel Colina¹ and Michael O'Sullivan²

¹Energy Development Corporation, 38/F One Corporate Centre,

Julia Vargas corner Meralco Avenue, Ortigas Center, Pasig City, 1605, Philippines

²Department of Engineering Science, University of Auckland, Auckland 1142, New Zealand

colina.rn@energy.com.ph; m.osullivan@auckland.ac.nz

Keywords: *geothermal reservoir modeling, calibration, inverse modeling, PEST.*

ABSTRACT

The natural state model of a geothermal reservoir numerically represents the state of the reservoir prior exploitation. Starting with an existing natural state model that gives a generally good match between simulated and measured down-well temperatures, inverse modeling is conducted to further improve the model. The inverse modeling software PEST is used to automatically calibrate the model. PEST utilizes advanced regularization and singular value decomposition techniques to ensure the numerical stability of the inversion process.

Permeability values of the reservoir rock are used as parameters that PEST automatically adjusts so that the difference between the measured and the simulated temperature is reduced. Significant improvement in the match to the measured temperatures is achieved after several optimization runs.

1. INTRODUCTION

The manual calibration of a reservoir model is a complicated and time-consuming task. Recently, automatic model calibration has been made possible with the implementation of inverse modeling techniques in codes such as iTOUGH2 (Finsterle and Pruess, 1999) and PEST (Doherty, 2010).

The inverse modeling technique involves estimation of model parameters by fitting the simulated model response to data measurements. In applying inverse modeling to the calibration of a geothermal reservoir model, the typical parameters are rock permeability, porosity, amount of mass and heat injected in the reservoir and productivity indices of the wells. Adjustments to these parameters are made until the model response matches the measured data, e.g. down-hole temperature, enthalpies or pressures. In this study the only model parameters used for calibration are the rock permeabilities which are automatically adjusted such that the simulated temperature closely matches the measured temperatures.

Finsterle and Pruess (1999) presented an optimization code called iTOUGH2 that allows estimation of any input parameter for a model based on the TOUGH2 reservoir simulator (Pruess, 1999). The computationally intensive inversion process involves many forward runs; however, as the runs are independent of each other, the process can be parallelised. There have been several applications of iTOUGH2 to the calibration of geothermal models (e.g.: White, 1995; Finsterle *et al.*, 1997; Kiryukhin *et al.*, 2008; Kumamoto *et al.*, 2008).

Cui *et al.* (2006) used a mathematical method called Markov chain Monte Carlo to automate the calibration process for a geothermal model. They showed that sample based inference provided a robust but time-consuming calibration approach.

There is not much published work on the use of PEST for geothermal model calibration. Shook and Renner (2002) coupled PEST with TETRAD, a reservoir simulator, to match the tracer and temperature histories of a hypothetical 2D model. The study conducted by Omagbon & O'Sullivan (2011) used PEST for automatic calibration of a reservoir model, using AUTOUGH2 as the simulator, the version of TOUGH2 used at the University of Auckland (Yeh *et al.*, 2012). That study implemented a heuristic approach for model structure refinement (Omagbon & O'Sullivan, 2011).

2. NATURAL STATE MODEL

The natural state model numerically represents the state of the reservoir prior field exploitation. An existing natural state model that provides a generally good match between simulated and measured temperatures is used in this study. Selected temperature profiles generated from this baseline model are shown in the Appendix.

The natural state model is configured such that the top of the model is set at the estimated depth of the water table. The maximum elevation of the model is 250mRSL. The thickness of the layers increases from 50m at the top of the model to 100m below -500mRSL. Below -1200mRSL, the thickness increases to 200m as shown in Figure 1.

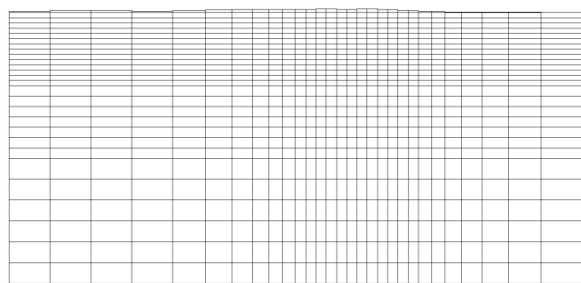


Figure 1. Vertical slice through the model grid

The model has 27486 blocks including one block to represent the atmosphere. It is assumed that the model is a closed system and, thus, no mass recharge occurs through the lateral boundaries.

3. MODEL CALIBRATION PROCESS WITH PEST

Model calibration is a necessary step to improve the fit of the simulated model results with the measured data. Calibration is commonly done manually which is generally a time-consuming process. In principle the model calibration problem can be solved by inverse modelling

techniques that allow automatic calibration of parameters. However, in practice, many problems arise in inverse modelling. The present paper outlines a case study of the application of inverse modelling to a natural state geothermal model and discusses the problems that were encountered. PEST, rather than iTOUGH2, was used in this study as it provides greater flexibility in controlling the inverse modelling process.

PEST is a model independent, inverse modelling code developed by Watermark Numerical Computing (Doherty, 2010). Using PEST, the objective is to reduce the difference between the simulated model results (down-hole temperatures in this case) and the measured values. The weighted sum of squared differences between the simulated temperatures and the measured temperatures is called the objective function. The aim of a PEST simulation is to reduce the value of the objective function thus improving the fit of the model to the data.

In order to use PEST for model calibration, several PEST text-based files are initially prepared: a template file, an instruction file and a PEST control file.

During the model calibration process, PEST must be able to write parameter values to the model input file for every forward run of AUTOUGH2. This is achieved by setting up a model template file that identifies the locations for the parameter values that PEST will change during calibration.

The results from a single forward run from AUTOUGH2 is written to a LISTING file. Using PyTOUGH (Croucher, 2011), the simulated temperatures are extracted from the LISTING file and saved as a simpler DAT file. An instruction file is prepared to tell PEST the location of the simulated values in the DAT file that it must read to compare with the corresponding measured values.

The parameter estimation process is controlled in the PEST control file. This file contains information such as the number of optimisation required, the complete list of parameters to adjust, the type of parameter transformation to use, parameter bounds, etc. Recommended values for many of the variables that must be supplied in the PEST control file can be found in the PEST manual. The detailed procedure for preparing the PEST files can be found in the PEST manual (Doherty, 2010) and at the PEST website (<http://www.pesthomepage.org/>).

Potentially, the x, y, and z-permeability of each rock-type in the model could be included as parameters for optimisation, for our model giving a total of 372 parameters to be estimated by PEST (or 248 if the x and y permeabilities are taken to be equal). Such a large number of parameters may cause numerical instability in the optimisation process. A PEST option called regularisation is implemented in this study. Regularisation works by supplying supplementary information allowing simultaneous estimation of a large number of parameters without incurring numerical instability that normally accompanies parameter nonuniqueness (Doherty, 2010). The truncated singular value decomposition (truncated SVD), another method of inverse problem regularisation, is also implemented. It simplifies the inverse problem by estimating combinations of parameters rather than the parameters themselves. These two regularisation methods have strengths and weaknesses that are discussed in detail in the PEST manual (Doherty, 2010).

The calibration of the model was carried out using the PEST utility called SVD-assist (SVDA) that combines the strength of the two regularisation methods and eliminates their weaknesses (Doherty, 2010). Using SVDA means the calibration process is based on “super parameters” that are linear combinations of the base parameters (the original rock-type permeabilities). A key feature of SVDA is that it keeps the group of super parameters that influence the objective function and discards the super parameters that do not influence the objective function (called the null space of the parameter space). Thus this PEST utility decreases the number of parameter to be varied and therefore the number of forward model runs required per iteration.

The ability of PEST to be run in parallel decreases the time necessary to complete the calibration process. The model can be run in parallel using Beopest, which shares the source code of PEST across a network of processors. A multi-core computer was used to execute parallel PEST optimisations. Typically a forward run of the model took at least 3 hours to complete. The number of forward runs per optimisation iteration depends on the number of adjustable parameters. Thus, having 248 adjustable parameters requires 249 forward runs which would have taken an impractically large time to finish had we not run PEST in parallel.

4. RESULTS AND DISCUSSION

A total of 124 parameter groups are used in the model calibration with each group corresponding to a specific rock-type. The permeability in the y-direction is made the same as the permeability in the x-direction and thus the total number of adjustable parameters for this calibration is 248. The field has 16 wells and the measured temperatures from each well are grouped into so-called observation groups.

The number of optimisations to be carried out is initially set to zero, which terminates the process after only one forward model run. This enables a check of the PEST-model interface and provides the initial value of the objective function, including the contribution of each observation group to the objective function. Results showed that some observation groups dominate or contribute more to the objective function than other groups. A greater contribution to the objective function indicates a worse match between the simulated and the measured data. The contribution to the objective function is also dependent on the number of observation data (temperature data points to compare) for each observation group. The contribution of each observation group to the objective function can be made equal, irrespective of the number of observation data, by using the PEST utility PWTADJ1 and this option was applied in the present study.

The regularisation process requires a Jacobian file that contains the derivatives of each observation with respect to each parameters. This Jacobian file is calculated by setting the number of optimisations to -1. Regularisation is added by using the PEST utility ADDREG1 (Doherty, 2010). Another PEST utility called SUPCALC is used to determine the number of super parameters to be used in the optimisation.

The value of the objective function prior to model optimisation with PEST was 16000. After five optimisation iterations, including SVDA, the objective function was reduced to 9030. Based on this reduction of the objective

function, it can be expected that the temperature matches are significantly improved. The optimisation results are recorded in the REC file. The PEST simulation took 5 days to run on a 32 processor Windows cluster of the Energy Development Corporation (EDC).

Significant trial and error was involved before a successful PEST calibration was achieved. In the initial runs, only a few rock-types were used as parameters for optimisation. One trial used only two rock-types as parameters for estimation. In another trial, rock-types that are not frequently assigned to blocks were removed as parameters. After several trials, it was observed that for this particular model, using a few rock-types for optimisation did not significantly improve the temperature matches. Thus it was decided that all the rock-types in the model should be included as parameters for optimisation, even if it increased the time necessary to complete the calibration. However, Beopest was able to run the forward model in parallel and reduce the calibration time.

Some initial trouble-shooting was required when the PEST files were being set up. The instruction file had to be revised a several times to ensure that it pointed to the correct location of the simulated values. The template file had to be reviewed prior to each trial to ensure that the required format for TOUGH2 was maintained and the correct TOUGH2 parameters for the model were used. It was also a tedious task making sure that all the variables in the PEST control file were properly filled in.

The results of model calibration for a selected number of wells are shown in the Appendix. There is a clear improvement in the temperature matches of these wells.

The measured temperature profile for Well 1 is similar to the simulated profile of the baseline model (Figure A-1). However, as shown in Figure A-2, the match is improved in the calibrated model, especially at -550mRSL where a temperature reversal is observed. The simulated temperature shows conductive heating from -1300mRSL down to the bottom of the well and corresponds to a decrease in permeability below -1500mRSL (Figure 2).

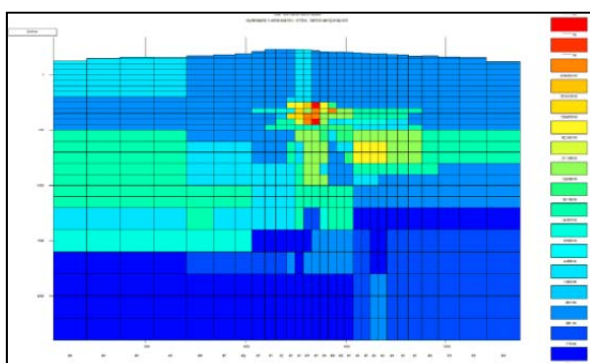


Figure 2 Vertical slice of the calibrated model showing the horizontal permeability structure

The temperature profile from the baseline model and the optimised model for Well 2 generally looks the same. However, when plotted against the measured temperature, the optimised model gives a better match.

For Well 6, the baseline model gives a good match with the measured temperature above -500mRSL (Figure C-1). However, below -500mRSL, the simulated temperature

starts to deviate from the measured data. The result of the optimised model for Well 6 shows an improved match (Figure C-2).

Comparing the results for the baseline model with the optimised model for Well 7 (Figures D-1 and D-2) showed that a significant improvement in the temperature match is achieved between -275mRSL and -750mRSL after the optimisation. However, below -750mRSL, the measured increase in temperature is not captured by the model. The assigned rock types in this area must be reviewed. The rock type maybe split into sub-types and allow PEST to recalibrate the model.

The optimised model gives a significantly better temperature match for Well 13 especially at -300mRSL to -500mRSL as shown in Figure E-2.

The baseline model resulted in a generally good match for the Well 14, especially at depths above -200mRSL. The simulated temperature from the baseline model, however, is much colder than the measured temperature from -200mRSL to -1000mRSL (Figure F-1). The optimised model was able to improve the temperatures for this section of the well, as shown in Figure F-2, by tightening the permeability in the area and preventing colder fluid into the well.

5. CONCLUSION AND RECOMMENDATIONS

Based on the temperature matches from the optimised model, it has been clearly established that PEST can be an effective tool for model calibration. Although the optimised temperature profiles do not exactly match the measured data, they are a significant improvement on those from the manually calibrated baseline model.

During model calibration, it was found that setting realistic lower and upper bound values for the parameters is very important. Initially a wide range of bounds was set and some permeability values became unrealistically low (e.g. ~0.05mD). The range of permeability values and the resulting optimised permeability determined by PEST should be reviewed by the modeller to ensure that the results are consistent with the geological information.

Based on the improvement in the natural state model, the next logical step to undertake is to proceed to production history matching. Although, experience tells us that a good natural state model does not necessarily mean we already have a good production model, the optimised natural state model is a good starting point for production history matching.

ACKNOWLEDGEMENTS

The authors would like to acknowledge the management of Energy Development Corporation for their support in finishing this paper.

REFERENCES

- Croucher, A.E., (2011). PyTOUGH: a Python scripting library for automating TOUGH2 simulations.
- Cui, T., Fox, C., Nicholls, G., & O'Sullivan, M. (2006). Bayesian Inference for Geothermal Model Calibration. *Proceedings 28th NZ Geothermal Workshop 2006*.

Doherty, J. (2010). "PEST: model-independent parameter estimation. User manual, 5th edition." Watermark Numerical Computing, Corinda, Australia, <http://www.sspa.com/pest>.

Finsterle, S., Pruess, K., Bullivant, D.P. & O'Sullivan, M.J. (1997). Application of inverse modeling to geothermal reservoir simulation. *Proceedings, Twenty-Second Workshop on Geothermal Reservoir Engineering*, Stanford University, Stanford, California, January 27–29, pp. 309–316.

Finsterle, S., & Pruess, K. (1999). Automatic Calibration of Geothermal Reservoir Models through Parallel Computing on a Workstation Cluster. *Proceedings, Twenty-Fourth Workshop on Geothermal Reservoir Engineering*. Stanford University, Stanford, California, January 25–27, pp. 123–130.

Kiryukhin, A.V., Asaulova, N.P. & Finsterle, S. (2008) Inverse modeling and forecasting for the exploitation of the Pauzhetsky geothermal field, Kamchatka, Russia, *Geothermics*, 37, 540–562, [doi:10.1016/j.geothermics.2008.04.003](https://doi.org/10.1016/j.geothermics.2008.04.003).

Kumamoto, Y., Itoi, R., Tanaka, T. & Hazama, Y. (2008). Development of the optimum numerical reservoir model of the Ogiri geothermal field, Kyushu, Japan, using iTOUGH2. *Proceedings, Thirty-Third Workshop on Geothermal Reservoir Engineering*, Stanford University, Stanford, California, January 28–30, pp. 1–8.

Newson, J. A., & O'Sullivan, M. J. (2009). Calibration of Mathematical Models for Heat and Mass Transfer in Thermal Soils. *Geothermal Resources Council Transactions*, 833–838. Davis, California.

Omagbon, J. B., & O'Sullivan, M. J. (2011). Use of an Heuristic Method and PEST for Calibration of Geothermal Models. *Proceedings 33rd New Zealand Geothermal Workshop*. Auckland, New Zealand.

O'Sullivan, M. J., Pruess, K., & Lippmann, M. J. (2000). Geothermal Reservoir Simulation: The State-of-practice and Emerging Trends. *Proceedings World Geothermal Congress 2000*. Japan.

Pruess, K., Oldenburg, K. & Moridis, G. (1999). *TOUGH2 user's guide, version 2.0*. Lawrence Berkeley National Laboratory, University of California, Berkeley.

Shook, G. M., & Renner, J. L. (2002). An Inverse Model for TETRAD: Preliminary Results. *Geothermal Resources Council*, 26, 119–122. Davis, California.

White, S.P. (1995). Inverse modeling of the Kawerau geothermal reservoir, New Zealand. *Proceedings 17th New Zealand Geothermal Workshop*. Auckland, New Zealand. 211–216.

Yeh, A., Croucher, A. & O'Sullivan, M.J. (2012), "Recent developments in the AUTOUGH2 simulator", Proceedings TOUGH Symposium 2012, Berkeley, California, September 17–19, 2012.

APPENDIX.

Comparison of temperature profiles between the baseline natural state model and the PEST optimized natural state model

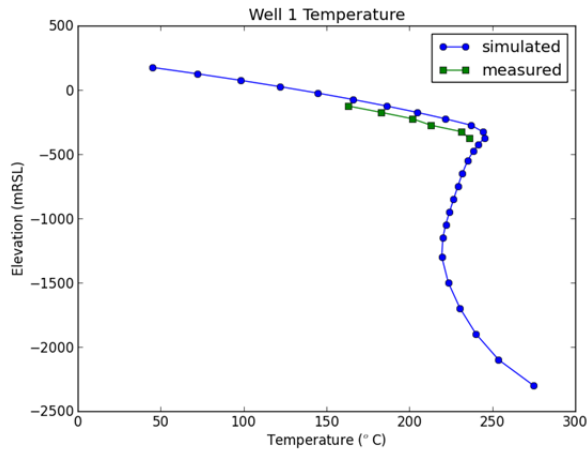


Figure A- 1. Well 1 temperature profile from the baseline model

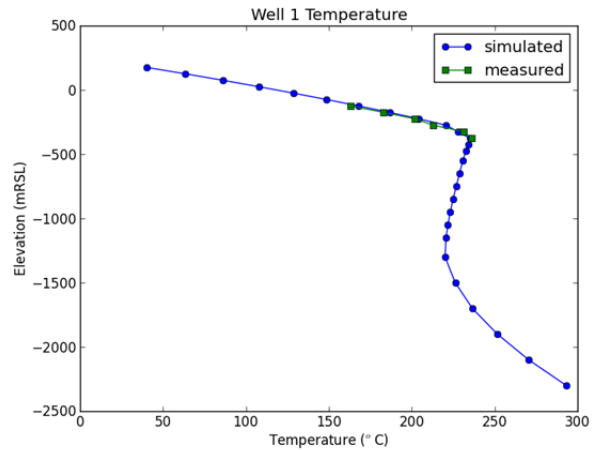


Figure A- 2. Well 1 temperature profile from the PEST optimized model

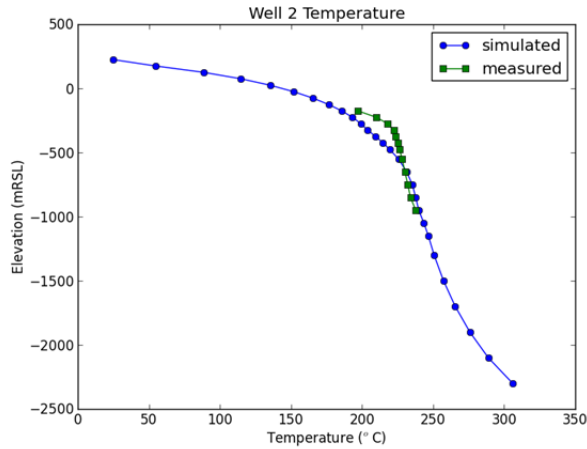


Figure B- 1. Well 2 temperature profile from the baseline model

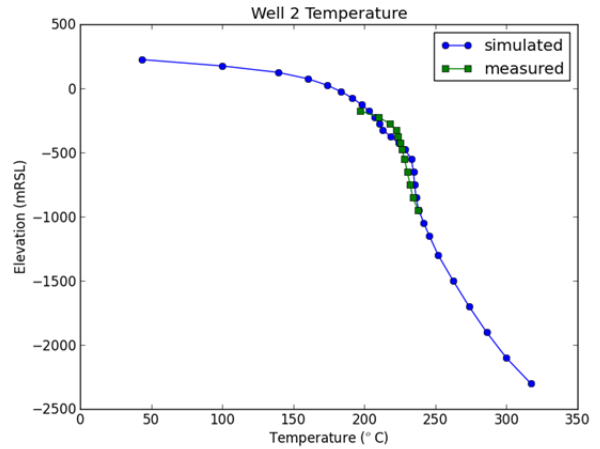


Figure B- 2. Well 2 temperature profile from the PEST optimized model

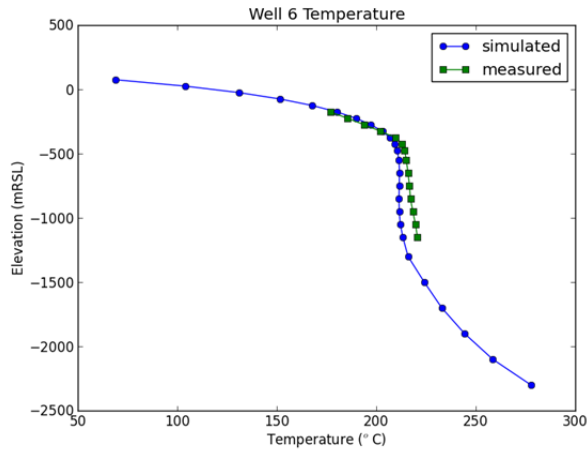


Figure C- 1. Well 6 temperature profile from the baseline model

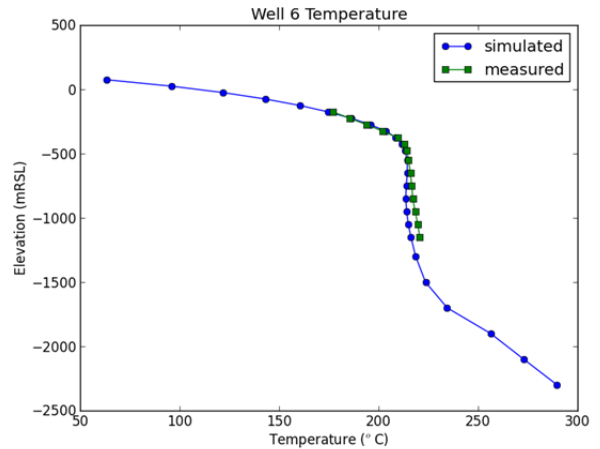


Figure C- 2. Well 6 temperature profile from the PEST optimized model

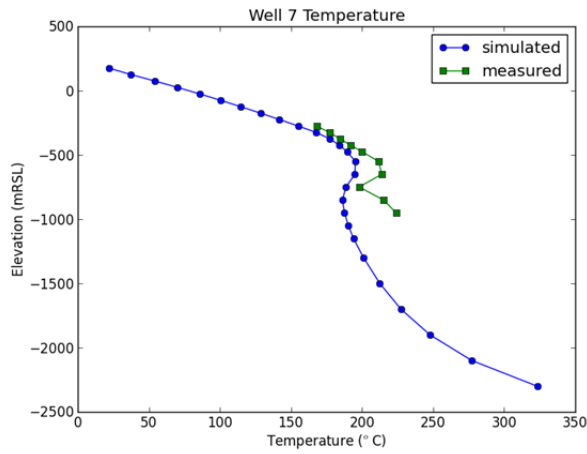


Figure D- 1. Well 7 temperature profile from the baseline model

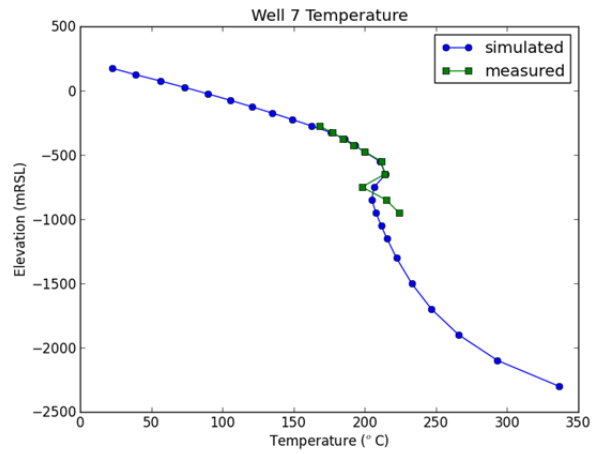


Figure D- 2. Well 7 temperature profile from the PEST optimized model

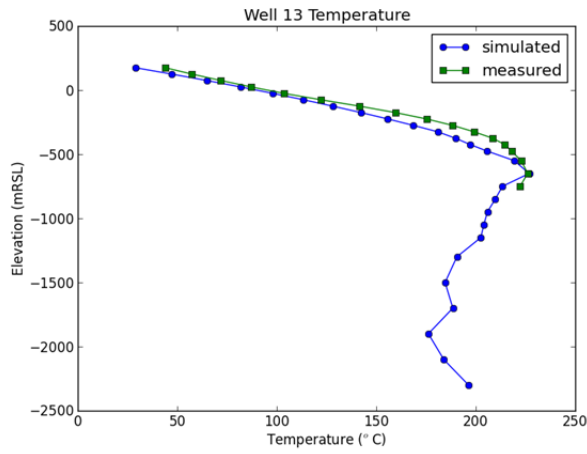


Figure E- 1. Well 13 temperature profile from the baseline model

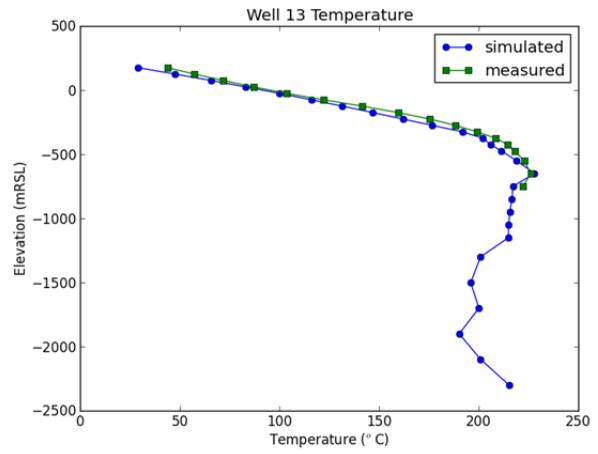


Figure E- 2. Well 13 temperature profile from the PEST optimized model

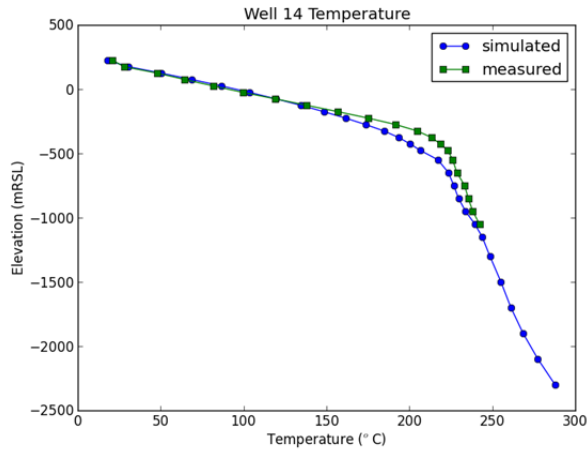


Figure F- 1. Well 14 temperature profile from the baseline model

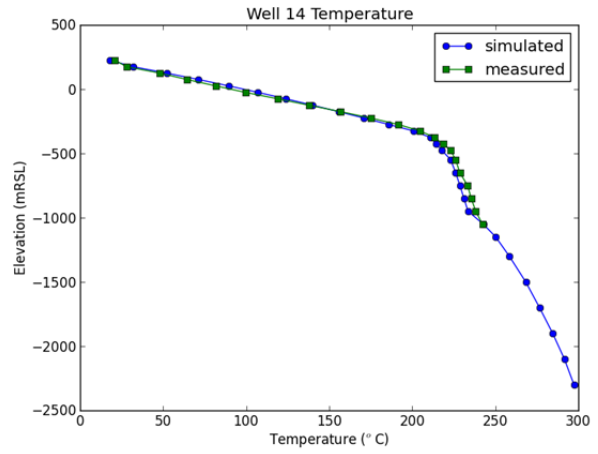


Figure F- 2. Well 14 temperature profile from the PEST optimized model